Chapter 5

# Gas Well Testing

Freddy Humberto Escobar

Additional information is available at the end of the chapter

http://dx.doi.org/10.5772/67620

**Abstract**

Modeling liquid flow for well test interpretation considers constant values of both density and compressibility within the range of dealt pressures. This assumption does not apply for gas flow case in which the gas compressibility factor is also included for a better mathematical representation. The gas flow equation is normally linearized to allow the liquid diffusivity solution to satisfy gas flow behavior. Depending upon the viscosity-compressibility product, three treatments are considered for the linearization: square of pressure squared, pseudopressure, or linear pressure. When wellbore storage conditions are insignificant, drawdown tests are best analyzed using the pseudopressure function. Besides, since the viscosity-compressibility product is highly sensitive in gas flow; then, pseudotime best captures the gas thermodynamics. Buildup pressure tests, for example, require linearization of both pseudotime and pseudopressure. The conventional straight-line method has been customarily used for well test interpretation. Its disadvantages are the accuracy in determining of the starting and ending of a given flow regime and the lack of verification. This is not the case of the Tiab's Direct Synthesis technique (*TDS*) which is indifferently applied to either drawdown or buildup tests and is based on features and intersection points found of the pressure and pressure derivative log-log plot.

**Keywords:** *TDS* technique, pseudotime, pseudopressure, rapid flow, viscosity, rate transient analysis, pressure transient analysis

## 1. Introduction

Contrary to liquids, a gas is highly compressible and much less viscous. In general, gas viscosity is about a 100 times lower than the least viscous crude oil. It is important, however, to try to provide the same mathematical treatment to oil and gas hydrocarbons, so interpretation methodologies can easily be applied in a more practical way. Then, the gas flow equation is normally linearized to allow the liquid diffusivity solution to satisfy the gas behavior when analyzing transient test data of gas reservoirs. Depending on the values of reservoir pressure, viscosity, and

gas compressibility factor, the gas flow behavior can be treated as a function of either pressure to the second power or linear pressure with a region which does not correspond to any of these and it is better represented by a synthetic function call pseudopressure. Pseudopressure is a function that integrates pressure, density, and compressibility factor. The gas system's total compressibility highly depends on gas compressibility which for ideal gases changes inversely with the pressure. Then, another artificial function referred as pseudotime is included to further understand the transient behavior of gas flow in porous media. For instance, when wellbore storage conditions are insignificant, drawdown tests are best analyzed using the pseudopressure function. On the other hand, buildup pressure tests require linearization of both pseudotime and pseudopressure.

This chapter will be devoted to provide both fundamental of gas flow in porous media as well as interpretation of pressure and rate data in gas reservoirs. The use of the oil flow equations and interpretation techniques is carefully extended for gas flow so that reservoir permeability, skin factor, and reservoir area can be easily estimated from a gas pressure or gas rate test by using conventional analysis and characteristic points found on the pressure derivative plot (*TDS* technique). Conventional analysis—the oldest pressure transient test interpretation technique—is based upon understanding the flow behavior in a given reservoir geometry, so the pressure versus time function is plotted in such way that a linear trend can be obtained. Both slope and intercept of such linear tendency are used to characterize the reservoir. Conventional analysis has two main drawbacks: (1) difficulty of finding a given flow regime and (2) absence of parameter verification. On the other hand, *TDS* technique—is strongly based on the log-log plot of pressure and pressure derivative versus time curves which provide the best way for flow regime identification; then, it uses the "fingerprints" or characteristic points found in such plot which are entered in practical and direct analytical equations to easily find reservoir parameters. Moreover, the same parameters can be obtained from different sources for verification purposes. Such is the case, for instance, of the reservoir area in elongated systems which can be estimated five times.

The chapter will include both interpretation techniques *TDS* and conventional in two cases: (1) infinite and (2) finite reservoirs. Channels or elongated systems in which reservoir hemilinear, parabolic or linear flow regimes developed once radial flow regime vanishes are reported in Refs [8, 13, 14]. This formation of linear flow regime normally occurs in fluvial deposits (channels), sand lens, parallel faulting, terrace faulting, and carbonate reefs. Then, such systems are worth of transient pressure analysis characterization. Latest researches on the determination of drainage area in constant-pressure-bounded systems using either conventional analysis or *TDS* technique are also reported by Escobar et al. [10].

It is convenient to mention some other important aspects concerning gas well testing which have appeared recently. The first case is the transient rate analysis in hydraulically fractured wells which was presented by [19] for both oil and gas wells. The traditional model for elliptical flow included the reservoir area as a variable. Handling the interpretation using *TDS* Technique may be little difficult for unexperienced interpreters. Therefore, [20] introduced a model excluding the reservoir drainage area and avoiding the necessity of developing pseudosteady-state regime. When a naturally fractured reservoir is subjected to hydraulic fracturing, the interpretation should be performed according to the presented by [21]. [35]

presented the pressure behavior of finite-conductivity fractured wells in gas composite systems. As far a horizontal wells, the recent works by [23] and [24] included off-centered wells for transient-rate or transient-pressure cases, respectively. [29] presented a study of production performance of horizontal wells when rapid flow conditions are given.

Practical exercises will provide in the chapter provide a better understanding and applicability of the interpretation techniques.

The purpose of this chapter is two folded: (1) to present the governing equation for gas flow used in well test interpretation and (2) to use both conventional and *TDS* Techniques as valuable tools for well test interpretation in both transient rate and transient pressure analysis. Some detailed examples will be given for demonstration purposes.

## 2. Transient pressure analysis

Transient pressure analysis is performed measuring the bottom-hole pressure while the flow rate is kept constant.

### 2.1. Fluid flow equations

The gas diffusivity equation in oil-field units is given by:

$$\frac{1}{r}\frac{\partial}{\partial r}\left(\frac{P}{\mu(P)Z(P)}r\frac{\partial P}{\partial r}\right)=\frac{\phi}{0.0002637}\frac{\partial}{\partial t}\left(\frac{P}{Z(P)}\right) \tag{1}$$

Which can be modified to respond for three-phase flow (oil, water, and gas):

$$\frac{1}{r}\frac{\partial}{\partial r}\left(r\frac{\partial P}{\partial r}\right)=\frac{\phi c_t}{0.0002637\lambda_t}\frac{\partial P}{\partial t} \tag{2}$$

where, the total compressibility, $c_t$, and total mobility, $\lambda_t$, are given by:

$$c_t \approx c_g s_g + c_o S_o + c_w S_w + c_f \tag{3}$$

$$\lambda_t = \frac{k_g}{\mu_g}+\frac{k_o}{\mu_o}+\frac{k_w}{\mu_w} \tag{4}$$

As can be inferred from Eq. (3), the total compressibility varies significantly when dealing with monophasic gas flow since the gas compressibility varies along with the pressure. Agarwal [1] introduced the pseudotime function to alleviate such problem. This function accounts for the time dependence of gas viscosity and total system compressibility:

$$t_a = \int_{t_{ref}}^{t}\frac{dt}{\mu(t)c_t(t)} \tag{5}$$

Pseudotime is better defined as a function of pressure as a new function given in hr psi/cp:

$$t_a(P) = \int_{P_{ref}}^{P} \frac{(dt/dP)}{\mu(P)c_t(P)} dP \tag{6}$$

Notice that $\mu$ and $c_t$ are now pressure-dependent properties.

As expressed by Eq. (1), viscosity and gas compressibility factor are strong functions of pressure; then, to account for gas flow behavior, Al-Hussainy et al. [2] introduced the pseudopressure function which basically includes the variation of gas viscosity and compressibility into a single function which is given by:

$$m(P) = 2\int_{P_{ref}}^{P} \frac{P}{\mu(P)Z(P)} dP \tag{7}$$

After replacing Eqs. (6) and (7) into Eq. (1), it yields:

$$\frac{1}{r}\frac{\partial}{\partial r}\left(r\frac{\partial m(P)}{\partial r}\right) = \frac{\phi}{0.0002637k}\frac{\partial m(P)}{\partial t_a(P)} \tag{8}$$

Contrary to liquid well testing, rapid gas flow has a strong influence on well testing, [32]. As the flow rate increases, so does the skin factor, then:

$$s_a = s + Dq \tag{9}$$

Eq. (9) shows that the apparent skin factor is a function of the mechanical skin factor—which is assumed to be constant during the test— and the product of the flow rate with the turbulence factor or non-Darcy term. This implies that two flow test ought to be run at different flow rates to find mechanical skin factor and the turbulence factor from:

$$(s_a)_1 = s + Dq_1 \tag{10}$$

$$(s_a)_2 = s + Dq_2 \tag{11}$$

Solving the simultaneous equations:

$$D = \frac{(s_a)_1 - (s_a)_2}{q_1 - q_2} \tag{12}$$

$$s = (s_a)_1 - \frac{(s_a)_1 - (s_a)_2}{q_1 - q_2} q_1 \tag{13}$$

where, the skin factors 1 and 2 are estimated from each pressure test. However, there is a need of estimating the turbulence factor by empirical correlations for buildup cases or when a single test exists. Then, the non-Darcy flow coefficient is defined by [26]:

http://dx.doi.org/10.5772/67620

$$D = 2.222 \times 10^{-15} \frac{\gamma_g k h \beta}{\mu_g r_w h_p^2} \tag{14}$$

The above equation is also applied to partially completed or partially penetrated wells. $h_p$ is the length of the perforated interval. For fully perforated wells, $h_p = h$.

Parameter $\beta$ is called turbulence factor or inertial factor can be found by correlations. The correlation proposed by Geertsma [21] is given by:

$$\beta = \frac{4.851 \times 10^4}{\phi^{5.5}\sqrt{k}} \tag{15}$$

The consideration on the skin factor effect on gas testing was recognized by Fligelman et al. [25] who provided correction charts to account for apparent skin factor values.

### 2.2. Conventional analysis

The solution to the transient diffusivity equation, Eq. (8), is given by:

$$m(P)_D(1, t_{Da}) = -\frac{1}{2} Ei\left(-\frac{1}{4t_{Da}}\right) \tag{16}$$

The dimensionless parameters used in this chapter are given below. The rigorous dimensionless time is:

$$t_D = \frac{0.0002637kt}{\phi(\mu c_t) r_w^2} \tag{17}$$

Including the pseudotime function, $t_a(P)$, the dimensionless pseudotime is:

$$t_{Da} = \left(\frac{0.0002637k}{\phi r_w^2}\right) t_a(P) \tag{18}$$

Notice that the viscosity-compressibility product is not seen in Eq. (16) since they are included in the pseudotime function. However, if we multiply and, then, divide by $(\mu c_t)_i$, a similar equation to the general dimensionless time expression will be obtained.

$$t_{Da} = \left(\frac{0.0002637k}{\phi(\mu c_t)_i r_w^2}\right)[(\mu c_t)_i \times t_a(P)] \tag{19}$$

The dimensionless pseudopressure and pseudopressure derivatives are:

$$t^* \Delta m(P)_D{}' = \frac{hk[t^* \Delta m(P)']}{1422.52 q_{sc} T} \tag{19a}$$

$$m(P)_D = \frac{hk[m(P_i) - m(P)]}{1422.52 q T} \tag{20}$$

$$t_a(P)^*\Delta m(P)_D{}' = \frac{hk[t_a(P)^*\Delta m(P)']}{1422.52q_{sc}T} \tag{21}$$

And the dimensionless wellbore storage coefficient is given by:

$$C_D = \left(\frac{0.8935}{\phi hc_t r_w^2}\right)C \tag{22}$$

The dimensionless radii are given:

$$r_D = \frac{r}{r_w} \tag{23}$$

$$r_{De} = \frac{r_e}{r_w} \tag{24}$$

For practical purposes, Eq. (16) will end up in a semilog behavior of pseudopressure drops against time. After replacing the respective dimensionless quantities into the mentioned straight-line semilog expression, it is obtained [4]:

$$m(P_i) - m(P_{wf}) = \frac{1.422 \times 10^6 qT}{kh}\left[1.1513\log\left(\frac{kt}{1688\phi(\mu_g c_t)_i {r_w}^2}\right) + s' + D\right] \tag{25}$$

$$m(P_i) - m(P_{wf}) = \frac{1.422 \times 10^6 qT}{kh}\left[1.1513\log\left(\frac{kt_a(P)}{1688\phi {r_w}^2}\right) + s' + D\right] \tag{26}$$

The above equations are applied during transient or radial flow regime. They are used to find reservoir transmissibility and apparent skin factor from the slope and intercept, respectively, of a semilog plot of well-flowing pressure versus time. After applying the superposition principle, the above equations for the buildup case are converted into:

$$m(P_i) - m(P_{wf}) = \frac{1.422 \times 10^6 qT}{kh}\log\left(\frac{t_p + \Delta t}{\Delta t}\right) \tag{27}$$

$$m(P_i) - m(P_{wf}) = \frac{1.422 \times 10^6 qT}{kh}\log\left(\frac{t_a(P)_p + \Delta t_a(P)}{\Delta t_a(P)}\right) \tag{28}$$

From a semilog plot of pseudopressure versus time (or pseudotime), its slope allows calculating the reservoir permeability and the intercept is used to find the pseudoskin factor, respectively:

$$k = \frac{1637.74qT}{mh} \tag{29}$$

$$s' = \left[\frac{m(P_i) - m(P_{1hr})}{m} - \log\left(\frac{k}{\phi(\mu c_t)_i r_w^2}\right) - 3.227 + 0.8686\right] \tag{30}$$

Notice that for the pseudotime case, $(\mu c_t)_i$ product in the above equation will be set as the unity. The gas pseudoskin factor is estimated for the buildup case as:

$$s' = \left[\frac{m(P_{1hr}) - m(P_{wf})}{m} - \log\left(\frac{k}{\phi(\mu c_t)_i r_w^2}\right) - 3.227 + 0.8686\right] \tag{31}$$

The governing dimensionless pressure equation during pseudosteady-state period is given by [28]:

$$m(P)_D = \frac{2t_D}{r_{eD}^2} + \ln r_D - 0.75 + s' \tag{32}$$

By replacing the dimensionless quantities, changing the log base, the above equation leads to:

$$m(P_i) - m(P_{wf}) = \frac{0.2395qTt}{Ah\phi} + \frac{3263qT}{kh}\left[\log\frac{0.472r_e}{r_w} + \frac{s'}{2.303}\right] \tag{33}$$

A Cartesian plot of $m(P_{wf})$ versus time or pseudotime during pseudosteady state will yield a straight line in which slope, $m^*$, is useful to find the well drainage area:

$$A = \frac{0.23395(5.615)qT}{\phi h m^*} \tag{34}$$

Such deliverability tests as backpressure, isochronal, modified isochronal, and flow after flow are conducted for the purpose of determining the flow exponent $n$ ($n$ = 1 is considered turbulent flow and $0.5 < n < 1$ is considered to be rapid flow) and the performance coefficients. They assumed that stabilization is reached during the testing which is not true in most of the cases. Then, they are not included in this chapter but can be found in Chapter 4 of Ref. [4].

### 2.3. *TDS* technique

Tiab [33] proposed a revolutionary technique which is very useful to interpret pressure tests using characteristics points found on the pressure and pressure derivative versus time log-log plot. He obtained practical analytical solutions for the determination of reservoir parameters.

$$m(P)_{Dr} = \left(\frac{7.029 \times 10^{-4} kh}{qT}\right)\left(\frac{m(P_i) - m(P_{wf})(t_n)}{q_n}\right) = \frac{1}{2}(\ln t_D + 0.80907 + 2s) \tag{35}$$

From a log-log plot of pseudopressure and pseudopressure derivative against pseudotime, **Figure 1**, several main characteristics are outlined:

1. The early unit-slope line originated by wellbore storage is described by the following equation:

$$m(P)_D = \frac{t_{Da}}{C_D} \tag{36}$$

Replacing the dimensionless parameters in Eq. (36), a new equation to estimate the wellbore storage coefficient is obtained:

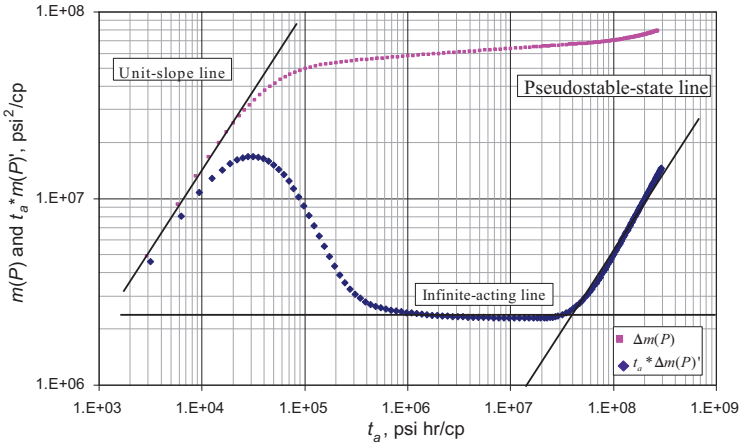


**Figure 1.** Log-log plot of pseudopressure and pseudopressure derivative versus pseudotime. After Ref. [7].

$$C = (0.419qTc_t)\left(\frac{t_a(P)}{\Delta m(P)}\right) \tag{37}$$

2. The intersection of the early unit-slope line with the radial horizontal straight line gives:

$$\left(\frac{t_{Da}}{C_D}\right)_i = 0.5 \tag{38}$$

From this, an equation to estimate either permeability or wellbore storage is obtained once the dimensionless parameters are replaced.

As presented by Tiab [33], the governing equation for the well pressure behavior during radial flow reformulated by Escobar et al. [7] in terms of pseudofunctions is expressed by:

$$t_a(P)_i = \frac{1695c_tC}{kh} \tag{39}$$

3. According to Ref. [28], another form of Eq. (35) is obtained when wellbore storage and skin factor are included:

$$m(P)_{Dr} = \frac{1}{2}\left\{\ln\left(\frac{t_{Da}}{C_D}\right)_r + 0.80907 + \ln(C_De^{2s})\right\} \tag{40}$$

From the above equation, the derivative of pseudopressure with respect to the natural log of $t_{Da}/C_D$ is given by:

$$\left[\frac{t_{Da}}{C_D}m(P)'_D\right]_r = 0.5 \tag{41}$$

From Eq. (21), the dimensionless pseudopressure derivative with respect to the natural log of log $t_{Da}/C_D$ gives:

http://dx.doi.org/10.5772/67620

$$\left[\frac{t_{Da}}{C_D} m(P)'_D\right]_r = \left[7.029 \times 10^{-4} \frac{kh}{qT}\right] [t_a(P) * m(P)'] \tag{42}$$

Combination of Eqs. (41) and (42) will result into an equation to estimate permeability:

$$k = \frac{711.26qT}{h[t_a(P) * \Delta m(P)']_r} \tag{43}$$

3. Dividing Eq. (40) by Eq. (41), replacing the dimensionless quantities and, then, solving for the pseudoskin factor will yield:

$$s' = 0.5\left[\frac{[\Delta m(P)]_r}{[t_a(P) * \Delta m(P)']_r} - \ln\left(\frac{k\left(t_a(P)\right)_r}{\phi r_w^2}\right) + 7.4316\right] \tag{44}$$

Finally, the pressure derivative during the pseudosteady-state flow regime of closed systems is governed by:

$$t_{Da} * m(P)'_D = 2\pi t_{Da} \tag{45}$$

The intersection point of the above straight line and the radial flow regime straight line is:

$$t_{aDARP_i} = \frac{1}{4\pi} \tag{46}$$

After substituting the dimensionless pseudotime function into Eq. (46), a new equation for the well drainage area is presented:

$$A = \frac{kt_a(P)_{rpi}}{301.77\,\phi} \tag{47}$$

Further applications of gas well test can be found in the literature. Escobar et al. [12] introduced the mathematical expressions for interpretation of pressure tests using the pseudopressure and pseudopressure derivative as a function of pseudotime for hydraulically fractured wells and naturally fractured (heterogeneous) formations. Fligelman [30] presented an interpretation methodology using *TDS* technique for finite-conductivity fractured wells. They used pseudopressure and rigorous time. In 2012, Escobar et al. [16] implemented the transient pressure analysis on gas fractured wells in bi-zonal reservoirs. Moncada et al. [31] extended the *TDS* for oil and gas flow for partially completed and partially penetrated wells. As far as horizontal wells, it is worth to mention the work performed in Refs. [11] and [15] on homogeneous and naturally fractured reservoirs.

### 2.4. Example 1

Chaudhry [4] presented a reservoir limit test for a gas reservoir (example 5-2 of Ref. [4]). However, once the pressure derivative was taken to the test data, no late pseudosteady state regime was observed. Then, the input data given below were used to simulate a pressure test given in **Table 1**.

| | | |
|---|---|---|
| $S_g$ = 70% | $S_w$ = 30% | $q$ = 6184 MSCF/D |
| $h$ = 41 ft | $k$ = 44 md | $B_g$ = 0.00102 $ft^3$/STB |
| $r_w$ = 0.4271 ft | $\phi$ = 10.04% | $c_t$ = 0.0002561 $psi^{-1}$ |
| $\omega_g$ = 0.0992 md/cp | $\gamma_g$ = 0.732 | $P_{cr}$ = 380.16 psia |
| $T_{cr}$ = 645.06 R | $T$ = 710 R | $r_e$ = 2200 ft (349 Ac) |
| $m(P_i)$ = 340920304.2 $psi^2$/cp | | |

| ***t*, hr** | ***P*, psi** | ***t*, hr** | ***P*, psi** |
|---|---|---|---|
| 0 | 3965 | 1.2713 | 3677.2527 |
| 0.001 | 3960.629 | 1.6005 | 3670.3779 |
| 0.002 | 3956.4313 | 2.0148 | 3663.602 |
| 0.003 | 3952.3774 | 2.5365 | 3656.8388 |
| 0.004 | 3948.4516 | 3.1933 | 3650.1477 |
| 0.005 | 3944.6431 | 4.0202 | 3643.5144 |
| 0.006 | 3940.9438 | 5.0107 | 3637.2126 |
| 0.007 | 3937.3469 | 6.0107 | 3632.0323 |
| 0.008 | 3933.8466 | 7.0107 | 3627.6664 |
| 0.009 | 3930.4382 | 8.0107 | 3623.8936 |
| 0.0113 | 3922.8277 | 9.0107 | 3620.5718 |
| 0.0143 | 3913.8402 | 10.0107 | 3617.6047 |
| 0.018 | 3903.2573 | 12.0107 | 3612.4479 |
| 0.0226 | 3891.1325 | 21.0107 | 3596.5482 |
| 0.0285 | 3877.5006 | 30.0107 | 3586.4447 |
| 0.0358 | 3862.4816 | 39.0107 | 3579.0231 |
| 0.0451 | 3846.2054 | 48.0107 | 3573.1536 |
| 0.0568 | 3829.2592 | 57.0107 | 3568.2967 |
| 0.0715 | 3812.1329 | 66.0107 | 3564.1453 |
| 0.09 | 3795.2335 | 75.0107 | 3560.4805 |
| 0.1133 | 3779.2686 | 84.0107 | 3557.2312 |
| 0.1271 | 3771.7594 | 93.0107 | 3554.3136 |
| 0.16 | 3757.7512 | 102.0107 | 3551.6672 |
| 0.2015 | 3745.1803 | 179.5107 | 3535.5164 |
| 0.2537 | 3734.0438 | 269.5107 | 3523.5847 |
| 0.3193 | 3724.1258 | 359.5107 | 3514.1663 |
| 0.402 | 3715.1658 | 449.5107 | 3505.545 |
| 0.5061 | 3706.8112 | 539.5107 | 3497.2804 |

http://dx.doi.org/10.5772/67620

| $t$, hr | $P$, psi | $t$, hr | $P$, psi |
|---|---|---|---|
| 0.6372 | 3698.9669 | 629.5107 | 3489.1576 |
| 0.8021 | 3691.489 | 719.5107 | 3481.0959 |
| 1.0098 | 3684.2741 | 809.5107 | 3473.056 |

| $t_a(P)$, psi-hr/cp | $\Delta m(P)$, psi$^2$/cp | $t_a(P)^* \Delta m(P)'$, psi$^2$/cp | $t_a(P)$, psi-hr/cp | $\Delta m(P)$, psi$^2$/cp | $t_a(P)^* \Delta m(P)'$, psi$^2$/cp |
|---|---|---|---|---|---|
| 0 | 0 | 0 | 45802.414 | 1870739.384 | 17533667.77 |
| 37.7745 | 270218.7615 | 265698.0159 | 57569.7648 | 1838960.003 | 17954428.54 |
| 75.5167 | 518758.6126 | 520866.1041 | 72365.7851 | 1815682.598 | 18369258.28 |
| 113.2278 | 751325.0471 | 767304.1906 | 90970.2467 | 1799003.726 | 18783428.06 |
| 150.9089 | 968476.5902 | 1005966.456 | 114363.6923 | 1786548.918 | 19193297.17 |
| 188.561 | 1172014.904 | 1237504.102 | 143779.3051 | 1774358.756 | 19599754.75 |
| 226.185 | 1362245.214 | 1462410.249 | 178978.2667 | 1766967.699 | 19986008.75 |
| 263.7817 | 1544967.139 | 1681099.321 | 214477.474 | 1764620.952 | 20303606.64 |
| 301.352 | 1713052.797 | 1893921.256 | 249946.7071 | 1752899.594 | 20571329.92 |
| 338.8966 | 1876882.193 | 2101169.292 | 285390.4587 | 1717299.587 | 20802733.84 |
| 426.2923 | 2225474.894 | 2563944.683 | 320812.0523 | 1692510.182 | 21006509.26 |
| 536.1368 | 2605002.302 | 3110507.871 | 356214.0473 | 1681851.999 | 21188553.27 |
| 674.1563 | 3004035.218 | 3754179.95 | 426967.5286 | 1725356.98 | 21505009.16 |
| 847.5255 | 3404366.431 | 4491744.317 | 744772.1706 | 1759676.341 | 22480949.29 |
| 1065.235 | 3781729.348 | 5321159.089 | 1061858.072 | 1799660.974 | 23101515.46 |
| 1338.5511 | 4101068.915 | 6235191.645 | 1378463.16 | 1769298.728 | 23557564.54 |
| 1681.5934 | 4335396.363 | 7226023.963 | 1694705.511 | 1759287.154 | 23918367.9 |
| 2112.0768 | 4462372.666 | 8257991.514 | 2010656.317 | 1770713.335 | 24217012.8 |
| 2652.2558 | 4463511.759 | 9301323.123 | 2326363.101 | 1736601.944 | 24472345.81 |
| 3330.0995 | 4300906.005 | 10331215.57 | 2641858.765 | 1709368.012 | 24697796.42 |
| 4180.8019 | 4056795.12 | 11304325.65 | 2957168.15 | 1701504.59 | 24897723.65 |
| 4684.3808 | 3917486.951 | 11762181.87 | 3272311.76 | 1711704.512 | 25077261.23 |
| 5880.9567 | 3569692.658 | 12616571.14 | 3587306.105 | 1744436.565 | 25240114.57 |
| 7383.6218 | 3191507.548 | 13383609.83 | 6295436.794 | 1821464.183 | 26234973.81 |
| 9271.202 | 2873762.477 | 14063387.95 | 9432920.282 | 2036512.441 | 26970809.17 |
| 11642.9004 | 2591188.809 | 14668995.81 | 12564795.27 | 2355209.644 | 27552034.83 |
| 14623.503 | 2366500.199 | 15216145.54 | 15691965 | 2740929.323 | 28084374.29 |
| 18369.9003 | 2197999.347 | 15726460.2 | 18814758.13 | 3212985.03 | 28594968.02 |
| 23079.3518 | 2076483.39 | 16205683.18 | 21933329.44 | 3695740.205 | 29097073.99 |
| 28999.9239 | 1985415.325 | 16662774.49 | 25047755.95 | 4195533.855 | 29595671.37 |
| 36443.5374 | 1918507.605 | 17104058.59 | 28158083.33 | 4703995.72 | 30093194.56 |

**Table 1.** Pressure, pseudopressure, time, and pseudotime data for example 1.

Estimate permeability, skin factor, and drainage area by both conventional analysis and *TDS* technique.

*2.4.1. Solution by conventional analysis*

**Figure 2** presents a semilog pressure of pseudopressure versus pseudotime. The slope and intercept of the radial flow regime straight line in such plot are given below:

$$m = -3995147.42\ (\text{psi}^2/\text{cp})/(\log \text{hr} - \text{psi/cp})$$

$$m(P)_{1\,\text{hr}} = 342125555.5\ \text{psi}^2/\text{cp}$$

Use of Eqs. (27) and (28) allows finding reservoir permeability and pseudoskin factor, respectively:

$$k = \frac{1637.74qT}{mh} = \frac{1637.74(6184)(710)}{(3995147.42)(41)} = 43.45\ \text{md}$$

$$s' = \left[\frac{340920304.25 - 342125555.5}{-3995147.42} - \log\left(\frac{43.45}{(0.1004)(0.4271^2)}\right) - 3.227 + 0.8686\right] = -0.5172$$

To find the well drainage area, the Cartesian plot given in **Figure 3** was built. Its slope, $m^*$ = 0.0914 (psi$^2$/cp)/(hr−psi/cp), is plugged into Eq. (34):

$$A = \frac{0.23395qT}{\phi h m^*} = \frac{0.23395(6184)(710)}{(0.1004)(41)(0.0914)(43560)} = 336.4\ \text{Ac}$$

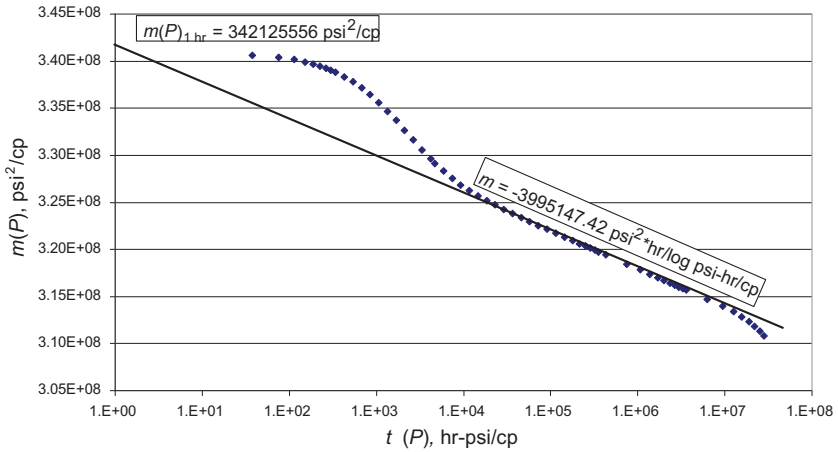


**Figure 2.** Semilog plot for example 1.

http://dx.doi.org/10.5772/67620

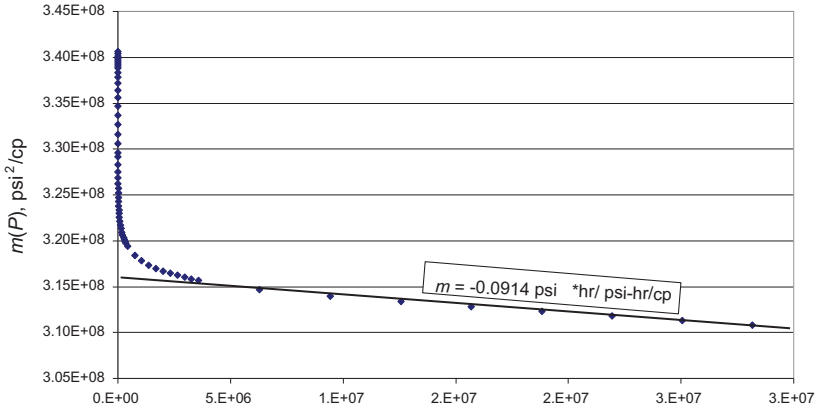


**Figure 3.** Cartesian plot for example 1.

### 2.4.2. *Solution by* TDS *technique*

**Figure 4** presents the pseudopressure and pressure derivative versus pseudotime log-log plot in which wellbore storage, radial flow regime, and late pseudosteady-state regimes are clearly observed. The following characteristic points were read from **Figure 4**:

| | |
|---|---|
| $t_a(P)_r$ = 1694705.5 psi hr/cp | $\Delta m(P)_r$ = 23918367.9 psi$^2$/cp |
| $t_a(P)^*\Delta m(P)'_r$ = 1735066.96 psi$^2$/cp | $t_a(P)_{rpi}$ = 10113641.48 psi hr/cp |

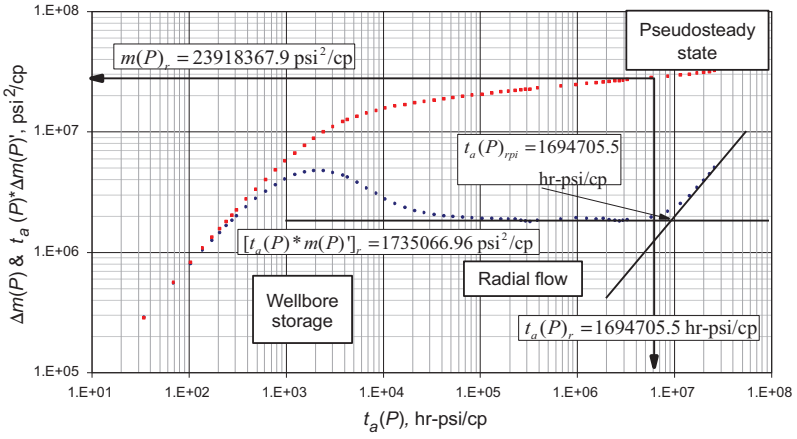


**Figure 4.** Pseudopressure drop and pseudopressure derivative versus time log-log plot for example 1.

Permeability and pseudoskin factor are respectively estimated from Eqs. (42) and (44),

$$k = \frac{711.26qT}{h[t_a(P) * \Delta m(P)']_r} = \frac{711.26(6184)(710)}{(41)(1735066.96)} = 43.9 \text{ md}$$

$$s' = 0.5\left[\frac{23918367.9}{1735066.96} - \ln\left(\frac{43.9(1694705.5)}{(0.1004)(0.4271^2)}\right) + 7.4316\right] = -0.454$$

and well drainage area is found with Eq. (47):

$$A = \frac{kt_a(P)_{rpi}}{301.77\,\phi} = \frac{(43.9)(10113641.48)}{301.77\,(0.1004)} = 336.4 \text{ Ac}$$

Finally, the inertial factor and the non-Darcy flow coefficient are estimated with Eqs. (14) and (15):

$$\beta = \frac{4.851 \times 10^4}{\phi^{5.5}\sqrt{k}} = \frac{4.851 \times 10^4}{(0.1004)\sqrt{43.9}} = 2265091235.63 \text{ ft}^{-1}$$

$$D = 2.222 \times 10^{-15}\frac{(0.732)(41)(43.9)(2265091235.63)}{(0.0992)(0.4271)(41^2)} = 9 \times 10^{-5} \text{ D/Mscf}$$

The true skin factor is found with Eq. (9):

$$s_a = s + Dq = -0.454 + 9 \times 10^{-5}\,(6184) = 1.42$$

It can be seen that the simulated parameters closely match the results obtained from the examples.

## 3. Transient rate analysis

Transient rate analysis is performed by recording the continuous changing flow rate under a constant bottom-hole pressure condition. This procedure is normally achieved in very low gas formations and shale gas systems.

### 3.1. Basic flow and dimensional equations

The Laplace domain, the rate of solution for a well producing against a constant bottom-hole well-flowing pressure was given by [34]:

$$q_D = \frac{1}{uK_0(\sqrt{u})} \tag{48}$$

The solution for a bounded reservoir was presented by [5]:

$$\overline{q}_D = \frac{I_1(r_{eD}\sqrt{u})K_1(\sqrt{u}) - K_1(r_{eD}\sqrt{u})I_1(\sqrt{u})}{\sqrt{u}[I_0(\sqrt{u})K_1(r_{eD}\sqrt{u}) + K_0(\sqrt{u})I_1(r_{eD}\sqrt{u})]} \tag{49}$$

http://dx.doi.org/10.5772/67620

For considerable longer times, Ref. [27] showed that the $q_D$ function in Eq. (48) may be approximated by:

$$\frac{1}{q_D} = \frac{1}{2}[\ln t_D + 0.80907] \tag{50}$$

where the dimensionless reciprocal rate and reciprocal rate derivative are given by:

$$1/q_D = \frac{k\,h\,\Delta m(P)}{1422.52\,Tq} \tag{51}$$

$$t_D * (1/q_D)' = \frac{k\,h\,[t * \Delta m(P)']}{1422.52\,Tq} \tag{52}$$

Including pseudoskin effects in Eq. (49),

$$\frac{1}{q_D} = \frac{1}{2}[\ln t_D + 0.80907 + 2s'] \tag{53}$$

### 3.2. Conventional analysis

After replacing the dimensionless quantities and changing the logarithm base, it yields:

$$\frac{1}{q} = \frac{1.422 \times 10^6 qT}{kh\Delta m(P)}\left[1.1513\log\left(\frac{kt_a(P)}{1688\phi r_w{}^2}\right) + s'\right] \tag{54}$$

As for the case of pressure transient analysis, from a semilog plot of pseudopressure versus time (or pseudotime), its slope allows calculating the reservoir permeability and the intercept is used to find the pseudoskin factor, respectively:

$$k = \frac{1637.74T}{mh\ \Delta m(P)} \tag{55}$$

$$s' = \left[\frac{(1/q)_{1hr}}{m} - \log\left(\frac{k}{\phi(\mu c_t)_i r_w^2}\right) - 3.227 + 0.8686\right] \tag{56}$$

Considering approximation for large time to the analytical Laplace inversion of Eq. (49), the following expression is obtained:

$$q_D = \frac{1}{\ln r_{eD} - 0.75}\exp\left[\frac{-2t_D}{r_{eD}^2(\ln r_{eD} - 0.75)}\right] \tag{57}$$

For $t_D \geq t_{Dpss}$, this flow period is known as the exponential decline period. $t_{Dpss}$ is the time required for the development of true pseudosteady state at the producing well for constant rate production case. Eq. (57) concerns only the circular reservoir. The solution can be generalized for other reservoir shapes by using the Dietz shape factor [6], $C_A$,

$$q_D = \frac{2}{\ln\left(\frac{4A_D}{\gamma C_A}\right)} \exp\left[\frac{-4\pi t_D}{A_D \ln\left(\frac{4A_D}{\gamma C_A}\right)}\right] \tag{58}$$

where, $A_D$ (dimensionless area) and $r_{eD}$ (dimensionless radius) are given by:

$$A_D = \frac{A}{r_w^2} \tag{59}$$

$$r_{eD} = \frac{r_e}{r_w e^{-s}} = \frac{r_e}{r_{weff}} \tag{60}$$

Eq. (58) suggests that a plot of log($q$) versus time will yield a straight line with negative slope $M_{decline}$,

$$M_{decline} = \frac{2(0.0002637)k}{r_{eD}^2(\ln r_{eD} - 0.75)\phi\mu c_t r_w^2} \tag{61}$$

and intercept at ($t$ = 0):

$$q_{\text{int}} = \frac{kh\Delta m(P)}{1637.74B\mu(\ln r_{eD} - 0.75)} \tag{62}$$

The reservoir area can be determined by solving the Eq. (62) for $r_{eD}$:

$$r_{eD} = \exp\left(\frac{1637.74B\mu}{kh\Delta m(P)(\ln r_{eD} - 0.75)} q_{\text{int}} + 0.75\right) \tag{63}$$

### 3.3. *TDS* technique

Escobar et al. [9] extended the *TDS* Technique for gas well in homogeneous and naturally fractured formations using rigorous time. The equations they presented for wellbore storage coefficient and permeability are given below:

$$C = 0.4196\frac{Tq\ t_N}{\mu\ \Delta m(P)_N} = 0.4198\frac{T}{\mu\,\Delta m(P)}\left[\frac{t}{t*(1/q)'}\right]_N \tag{64}$$

$$k = 711.5817\frac{T}{h\,\Delta m(P)[t\times(1/q)']_r} \tag{65}$$

Using a procedure similar to the pressure transient case, Escobar et al. [9] found an expression to estimate the pseudoskin factor:

$$s' = 0.5\left\{\frac{(1/q)_r}{[t\times(1/q)']_r} - \ln\left(\frac{kt_r}{\phi\,\mu\,c_t {r_w}^2}\right) + 7.43\right\} \tag{66}$$

For the estimation of reservoir area, Escobar et al. [9] also presented an equation that uses the starting time of the pseudosteady-state period, $t_{spss}$.

http://dx.doi.org/10.5772/67620

$$r_e{}^2 = \left(\frac{0.0015k\,t_{spss}}{\phi\mu\,c_t}\right)^{1/2} \tag{67}$$

As treated in pressure transient analysis, Eq. (41), the reciprocal rate derivative takes a value of 0.5 during radial flow. The intercept of this with the reciprocal rate derivative of Eq. (57) will provide:

$$t_{D_{rpi}} = \frac{1}{2} r_{eD}{}^2[\ln(r_{eD}) - 0.75] \tag{68}$$

in which numerical solution gives:

$$r_{eD} = 1.0292\ t_{D_{rpi}}^{0.4627} \tag{69}$$

After replacing the dimensionless quantities, we obtain:

$$r_e = 22.727 \times 10^{-3} r_{weff} \left(\frac{k}{\phi\,\mu\,c_t r_{weff}{}^2}\right)^{0.4627} t_{rpi}{}^{0.4627} \tag{70}$$

Refs. [13] and [14] presented rate transient analysis for long homogeneous and naturally fractured oil reservoirs using *TDS* technique and conventional analysis, respectively. Equations can be easily translated to gas flow.

### 3.4. Example 2

Escobar et al. [9] presented an example for a homogeneous bounded reservoir. **Figure 5** and **Table 2** present the reciprocal rate and reciprocal rate derivative versus rigorous time for this exercise. Other relevant data for this example are given below:

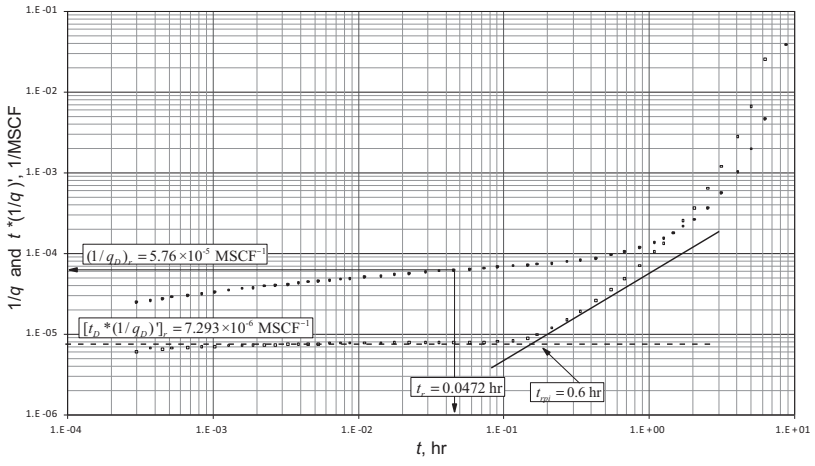


**Figure 5.** Reciprocal rate and reciprocal rate derivative for example 2—homogeneous bounded reservoir. After Ref. [9].

| | | |
|---|---|---|
| $h$ = 80 ft | $k$ = 25 md | $r_w$ = 0.3 ft |
| $\phi$ = 25% | $c_t$ = 0.00187 psi$^{-1}$ | $\mu_g$ = 0.0122 md/cp |
| $\gamma_g$ = 0.85 | $T$ = 670 R | $r_e$ = 30 ft (0.065 Ac) |
| $\Delta m(P)$ = 340920304.2 psi$^2$/cp | $\Delta P$ = 580 psi | |

Find reservoir permeability, skin factor, and drainage radius for this example using the *TDS* Technique.

| $t$, hr | $1/q$, MSCF$^{-1}$ | $t^*(1/q)'$, MSCF$^{-1}$ | $t$, hr | $1/q$, MSCF$^{-1}$ | $t^*(1/q)'$, MSCF$^{-1}$ |
|---|---|---|---|---|---|
| 3.11E-04 | 43189.24959 | 179751.1071 | 4.72E-02 | 17360.95346 | 135561.954 |
| 3.89E-04 | 40834.91569 | 162199.4397 | 6.09E-02 | 16811.48278 | 135417.1412 |
| 4.67E-04 | 39060.52002 | 163534.7645 | 7.58E-02 | 16365.45213 | 135450.8332 |
| 5.45E-04 | 37655.94848 | 160065.4877 | 0.094767643 | 15935.44127 | 134654.7122 |
| 7.01E-04 | 35537.19664 | 157149.8777 | 0.122175588 | 15464.07533 | 130033.9989 |
| 8.72E-04 | 33849.9472 | 154708.1815 | 0.152075165 | 15058.4209 | 120446.6934 |
| 1.07E-03 | 32361.46026 | 152593.8776 | 0.176991479 | 14766.60107 | 110524.7186 |
| 1.35E-03 | 30871.32659 | 150543.0499 | 0.224830802 | 14266.98732 | 91414.11215 |
| 1.66E-03 | 29601.36073 | 148839.1511 | 0.284629956 | 13699.34978 | 71972.81156 |
| 1.97E-03 | 28617.55908 | 147555.5061 | 0.354395635 | 13079.44168 | 55862.58323 |
| 2.36E-03 | 27646.46771 | 146325.5009 | 0.450074281 | 12279.66271 | 41400.85561 |
| 2.80E-03 | 26785.03603 | 145257.0868 | 0.569672588 | 11348.65545 | 30197.97654 |
| 3.42E-03 | 25823.21027 | 144105.0598 | 0.709203946 | 10349.64392 | 22079.63438 |
| 4.04E-03 | 25068.84401 | 143224.7896 | 0.900561238 | 9119.41797 | 15300.5905 |
| 4.73E-03 | 24398.17164 | 142461.4954 | 1.139757852 | 7783.903591 | 10316.16432 |
| 5.54E-03 | 23753.19888 | 141745.6607 | 1.315168702 | 6930.721305 | 7965.441894 |
| 6.63E-03 | 23056.85049 | 140996.5214 | 1.522472435 | 6043.090594 | 6009.327954 |
| 7.87E-03 | 22423.58559 | 140330.625 | 1.801535152 | 5027.292996 | 4239.056471 |
| 9.12E-03 | 21908.28203 | 139803.0353 | 2.120463971 | 4077.321632 | 2935.619806 |
| 1.15E-02 | 21141.51732 | 139045.8455 | 2.630750081 | 2923.310968 | 1712.191843 |
| 1.49E-02 | 20332.18915 | 138280.5426 | 3.28455416 | 1917.14852 | 909.5234175 |
| 1.86E-02 | 19683.45322 | 137688.6861 | 4.241340618 | 1040.993708 | 385.7970016 |
| 2.34E-02 | 19065.59817 | 137131.4759 | 5.261912839 | 543.216581 | 162.6885651 |
| 3.02E-02 | 18406.42719 | 136508.2532 | 6.569520997 | 230.4829168 | 41.88651512 |
| 3.77E-02 | 17872.96521 | 135981.9447 | 9.12095155 | 27.98082076 | 0.548915189 |

**Table 2.** Reciprocal rate, reciprocal rate derivative versus time data for example 2.

### *3.4.1. Solution*

The following characteristic points were read from **Figure 5**:

http://dx.doi.org/10.5772/67620

| | |
|---|---|
| $t_r = 4.72 \times 10^{-2}$ hr | $[t^*(1/q)']_r = 7.293 \times 10^{-6}$ D/Mscf |
| $(1/q)_r = 5.76 \times 10^{-5}$ D/Mscf | $t_{rpi} = 0.06$ hr |

Eqs. (65), (66), and (70) are used to obtain permeability, skin factor, and drainage.

$$k = \frac{711.5817T}{h\,\Delta m(P)[t \times (1/q)']_r} = \frac{711.5817(670)}{(80)(30976300)(7.293 \times 10^{-6})} = 26.37 \text{ md}$$

$$s' = 0.5\left\{\frac{(5.76 \times 10^{-5})}{(7.293 \times 10^{-6})} - \ln\left(\frac{(25)(0.0472)}{(0.25)(0.0122)(0.00187)(0.3)^2}\right) + 7.43\right\} = 0.68$$

$$r_e = 22.727 \times 10^{-3}(0.3)\left(\frac{(25)}{(0.25)(0.0122)\,(0.00187)(0.3)^2}\right)^{0.4627}(0.6)^{0.4627} = 19.5 \text{ ft}$$

Notice that the results closely match the permeability and external reservoir radius as presented by Ref. [9].

Finally, it is worth to mention that nowadays, conventional shale-gas reservoirs have become very attractive in the oil industry. Then, their characterization via well test analysis is very important. Shale-gas reservoir is normally tested under constant well-flowing pressure conditions—transient rate analysis—then, the recent studies performed in Refs. [17] and [22] should be read. If such wells are tested under constant rate conditions—pressure transient analysis—then the reader should refer to the works by Bernal et al. [3] and Escobar et al. [18].

## Nomenclature

| | |
|---|---|
| $A$ | Well drainage area, ft$^2$ and Ac |
| $B$ | Volumetric factor, rb/MSCF |
| $C$ | Wellbore storage coefficient, bbl/psi |
| $c_t$ | Total compressibility, 1/psi |
| $D$ | Turbulent flow factor, Mscf/D |
| $h$ | Formation thickness, ft |
| $h_p$ | Perforated interval, ft |
| $I_0$, $I_1$ | Bessel function |
| $k$ | Permeability, md |
| $K_0$,$K_1$ | Bessel function |
| $m$ | Semilog slope |
| $m^*$ | Cartesian slope |
| $m(P)$ | Pseudopropressure function, psi$^2$/cp |
| $M_{decline}$ | Slope of plot of log($q$) versus time |
| $n$ | Flow exponent |
| $P$ | Pressure, psi |

| | |
|---|---|
| $P_D$ | Dimensionless pressure |
| $P_{wf}$ | Well-flowing pressure, psi |
| $q$ | Gas flow rate, MSCF |
| $1/q$ | Reciprocal of the flow rate, D/Mscf |
| $r$ | Radius, ft |
| $r_e$ | External reservoir radius, ft |
| $r_w$ | Radio del pozo, ft |
| $r_{weff}$ | Effective wellbore radius, $r_w e^{-s}$, ft |
| $s'$ | Apparent or pseudoskin factor |
| $s_a$ | Total skin factor |
| $t$ | Time, hr |
| $t_D{*}P_D'$ | Dimensionless pressure derivative |
| $t_{Dpss}$ | Exponential decline period |
| $t{*}(1/q)'$ | Reciprocal rate derivative, D/Mscf |
| $t_D{*}(1/q_D)'$ | Dimensionless reciprocal rate derivative |
| $t_p$ | Horner or producing time |
| $t_{pss}$ | Exponential decline period, hr |
| $t_{spss}$ | Time to initiate pseudosteady state, hr |
| $u$ | Argument for a Bessel function |
| $Z$ | Gas supercompressibility factor |

## Greek

| | |
|---|---|
| $\alpha$ | Turbulence factor or inertial factor |
| $\Delta$ | Change, drop |
| $\phi$ | Porosity, fraction |
| $\gamma$ | Euler's constant—1.781 or $e^{0.5772}$ |
| $\gamma_g$ | Gas gravity |
| $\lambda$ | Mobility, md/cp |
| $\mu$ | Viscosity, cp |

## Suffices

| | |
|---|---|
| 1 *hr* | One hour |
| *cr* | Condition at critical point |
| *DA* | Dimensionless referred to drainage area |
| *Da* | Dimensionless referred to pseudotime |
| *D* | Dimensionless |
| *De* | Dimensionless referred to external |
| *e* | External |
| *eff* | Effective |
| *g* | Gas |

http://dx.doi.org/10.5772/67620

| | |
|---|---|
| *i* | Initial or intercept |
| *pss* | Pseudosteady state |
| *r* | Radial flow |
| *ref* | Reference |
| *rpi* | Intercept radial-pseudosteady |
| *t* | Total |
| $t_a(P)$ | Pseudotime, psi-hr/cp |
| *w* | Well |

## Author details

Freddy Humberto Escobar

Address all correspondence to: fescobar@usco.edu.co

Universidad Surcolombiana, Colombia

## References

[1] Agarwal, G., 1979. Real gas pseudo-time a new function for pressure buildup analysis of MHF gas wells. In 54th Technical Conference and Exhibition of the Society of Petroleum Engineers of AIME held in Las Vegas, NV, 23–26 September 1973.

[2] Al-Hussainy, R., Ramey, H.J. Jr., and Crawford, P.B. 1966. The flow of real gases through porous media. Journal of Petroleum Technology, Transactions AIME. 18:624–636.

[3] Bernal, K.M., Escobar, F.H., and Ghisays-Ruiz, A. 2014. Pressure and pressure derivative analysis for hydraulically-fractured shale formations using the concept of induced permeability field. Journal of Engineering and Applied Sciences. 9(10):1952–1958. ISSN 1819-6608.

[4] Chaudhry, A.U. 2003. Gas well testing handbook. Gulf Professional Publishing, Burlington, MA, USA, 887 p.

[5] Da Prat, G., Cinco-Ley, H., and Ramey, H. 1981, June 1. Decline curve analysis using type curves for two-porosity systems. Society of Petroleum Engineers. 21:354–362. doi:10.2118/9292-PA.

[6] Earlougher, R. C. 1971,October 1. Estimating drainage shapes from reservoir limit tests. Society of Petroleum Engineers. 23. pp. 1266–1268. doi:10.2118/3357-PA.

[7] Escobar, F.H., Lopez, A.M., and Cantillo, J.H. 2007, Decemeber. Effect of the pseudotime function on gas reservoir drainage area determination. CT&F—Ciencia, Tecnología and Futuro. 3(3):113–124. ISSN 0122-5383.

[8] Escobar, F.H., Hernández, Y.A., and Hernández, C.M. 2007. Pressure transient analysis for long homogeneous reservoirs using TDS technique. Journal of Petroleum Science and Engineering. 58(1–2):68–82. ISSN 0920-4105.

[9] Escobar, F.H., Sanchez, J.A., and Cantillo, J.H. 2008, December. Rate transient analysis for homogeneous and heterogeneous gas reservoirs using the TDS technique. CT&F—Ciencia, Tecnología y Futuro. 4(4):45–59.

[10] Escobar, F.H., Hernandez, Y.A., and Tiab, D. 2010, June.Determination of reservoir drainage area for constant-pressure systems using well test data. CT&F—Ciencia, Tecnología y Futuro. 4(1):51–72. ISSN 0122-5383.

[11] Escobar, F.H., Muñoz, Y.E.M., and Cerquera, W.M. 2011, September. Pressure and pressure derivate analysis vs. pseudotime for a horizontal gas well in a naturally fractured reservoir using the TDS technique. Entornos Journal. Issue (24):39–54.

[12] Escobar, F.H., Martinez, L.Y., Méndez, L.J., and Bonilla, L.F. 2012, March. Pseudotime application to hydraulically fractured vertical gas wells and heterogeneous gas reservoirs using the TDS technique. Journal of Engineering and Applied Sciences. 7(3):260–271.

[13] Escobar, F.H., Rojas, M.M., and Bonilla, L.F. 2012, March. Transient-rate analysis for long homogeneous and naturally fractured reservoir by the TDS technique. Journal of Engineering and Applied Sciences. 7(3):353–370. ISSN 1819-6608.

[14] Escobar, F.H., Rojas, M.M., and Cantillo, J.H. 2012, April. Straight-line conventional transient rate analysis for long homogeneous and heterogeneous reservoirs. Dyna. 79 (172):153–163. ISSN 0012-7353.

[15] Escobar, F.H., Muñoz, Y.E.M., and Cerquera, W.M. 2012. Pseudotime function effect on reservoir width determination in homogeneous and naturally fractured gas reservoir drained by horizontal wells. Entornos Journal. Issue (24):221–231.

[16] Escobar, F.H., Zhao, Y.L., and Zhang, L.H. 2014. Interpretation of pressure tests in hydraulically-fractured wells in bi-zonal gas reservoirs. Ingeniería e Investigación. 34 (4):76–84.

[17] Escobar, F.H., Montenegro, L.M., and Bernal, K.M. 2014. Transient-rate analysis for hydraulically-fractured gas shale wells using the concept of induced permeability field. Journal of Engineering and Applied Sciences. 9(8):1244–1254.

[18] Escobar, F.H., Bernal, K.M., and Olaya-Marin, G. 2014, August. Pressure and pressure derivative analysis for fractured horizontal wells in unconventional shale reservoirs using dual-porosity models in the stimulated reservoir volume. Journal of Engineering and Applied Sciences. 9(12):2650–2669.

[19] Escobar, F.H., Castro, J.R. and Mosquera, J.S. 2014, May. Rate-Transient Analysis for Hydraulically Fractured Vertical Oil and Gas Wells. Journal of Engineering and Applied Sciences. 9(5):739–749. ISSN 1819-6608.

[20] Escobar, F.H., Ghisays-Ruiz, A. and Bonilla, L.F. 2014, September. New Model for Elliptical Flow Regime in Hydraulically-Fractured Vertical Wells in Homogeneous and Naturally-Fractured Systems. Journal of Engineering and Applied Sciences. 9(9):1629–1636. ISSN 1819-6608.

[21] Escobar, F.H., Zhao, Y.L. and Fahes, M. 2015, July. Characterization of the naturally fractured reservoir parameters in infinite-conductivity hydraulically-fractured vertical wells by transient pressure analysis. Journal of Engineering and Applied Sciences. 10 (12):5352–5362. ISSN 1819-6608.

[22] Escobar, F.H., Rojas, J.D., and Ghisays-Ruiz, A. 2015, January. Transient-rate analysis hydraulically-fractured horizontal wells in naturally-fractured shale gas reservoirs. Journal of Engineering and Applied Sciences. 10(1):102–114. ISSN 1819-6608.

[23] Escobar, F.H., Pabón, O.D., Cortes, N.M., Hernández, C.M. 2016, September. Rate-transient analysis for off-centered horizontal wells in homogeneous anisotropic hydrocarbon reservoirs with closed and open boundaries. Journal of Engineering and Applied Sciences. 11(17):10470–10486. ISSN 1819-6608.

[24] Escobar, F.H., Cortes, N.M., Pabón, O.D., Hernández, C.M. 2016, September. Pressure-transient analysis for off-centered horizontal wells in homogeneous anisotropic reservoirs with closed and open boundaries. Journal of Engineering and Applied Sciences. 11 (17):10156–10171. ISSN 1819-6608.

[25] Fligelman, H., Cinco-Ley, H., and Ramey, H.J., Jr. 1981, March. Drawdown testing for high velocity gas flow. Paper SPE 9044 presented at the 1981 California Regional Meeting in Bakersfield, CA.

[26] Geertsma, J. 1974, October 1. Estimating the coefficient of inertial resistance in fluid flow through porous media. Society of Petroleum Engineers Journal. 14:445–450. doi:10.2118/4706-PA.

[27] Jacob, C.E., and Lohman, S. W. 1952, August. Non-steady flow to a well of constant drawdown in an extensive aquifer. Transactions American Geophysical Union. 559–569.

[28] Jones, P. 1962, June 1. Reservoir limit test on gas wells. Journal of Petroleum Technology. 14:613–619. doi:10.2118/24-PA.

[29] Lu, J., Li, S., Rahma, M.M. and Escobar, F.H. Escobar, F.H. and Zhang, C.P. 2016, August. Production Performance of Horizontal Gas Wells Associated with Non-Darcy Flow. 11 (15):9428–9435. ISSN 1819-6608.

[30] Nunez, W., Tiab, D., and Escobar, F.H. 2003, January,1. Transient pressure analysis for a vertical gas well intersected by a finite-conductivity fracture. Society of Petroleum Engineers. doi:10.2118/80915-MS.

[31] Moncada, K., Tiab, D., Escobar, F.H., Montealegre-M, M., Chacon, A., Zamora, R.A., and Nese, S.L. 2005, December. Determination of vertical and horizontal permeabilities for

vertical oil and gas wells with partial completion and partial penetration using pressure and pressure derivative plots without type-curve matching. CT&F—Ciencia, Tecnología y Futuro. 2(6):77–95.

[32] Ramey, H.J., Jr. 1965, February. Non-Darcy flow and wellbore storage effects in pressure buildup and drawdown of gas wells. Journal of Petroleum Technology. 17:223.

[33] Tiab, D. 1995. Analysis of pressure and pressure derivative without type-curve matching: 1-skin and wellbore storage. Journal of Petroleum Science and Engineering. 1995;12:171–181.

[34] Van Everdingen, A.F., and Hurst, W. 1949, December. The application of the Laplace transformation to flow problems in reservoirs. Society of Petroleum Engineers. 1. doi:10.2118/949305-G.

[35] Zhao, Y.L. Escobar, F.H., Hernandez, C.M., Zhang, C.P. 2016, August. Performance analysis of a vertical well with a finite-conductivity fracture in gas composite reservoirs. Journal of Engineering and Applied Sciences. 11(15):8992–9003. ISSN 1819-6608.